Chinese Chemical Letters 31 (2020) 2478–2482

Contents lists available at ScienceDirect

Chinese Chemical Letters

journal homepage: www.elsevier.com/locate/cclet

Communication

Pt nanodendrites with (111) crystalline facet as an efficient, stable and pH-universal catalyst for electrochemical hydrogen production

Huifang Sun[a,b,1], Qi Zeng[c,1], Chen Ye[b,d], Yangguang Zhu[b,e], Feiyue Chen[b,f], Mingyang Yang[b,d], Li Fu[g], Shiyu Du[h], Jinhong Yu[b,d], Nan Jiang[b,d], Jianxiong Liu[a,**], Tianzhun Wu[c,**], Cheng-Te Lin[b,d,*]

[a] Faculty of Materials Science and Engineering, Kunming University of Science and Technology, Kunming 650093, China
[b] Key Laboratory of Marine Materials and Related Technologies, Zhejiang Key Laboratory of Marine Materials and Protective Technologies, Ningbo Institute of Materials Technology and Engineering (NIMTE), Chinese Academy of Sciences, Ningbo 315201, China
[c] Shenzhen Institutes of Advanced Technology, Chinese Academy of Science, Shenzhen 518055, China
[d] Center of Material Science and Optoelectronic Technology, University of Chinese Academy of Sciences, Beijing 100049, China
[e] Laboratory of Environmental Biotechnology, School of Environmental and Civil Engineering, Jiangnan University, Wuxi 214122, China
[f] College of Science, Henan University of Technology, Zhengzhou 10463, China
[g] College of Materials and Environmental Engineering, Hangzhou Dianzi University, Hangzhou 310018, China
[h] Ningbo Institute of Materials Technology and Engineering (NIMTE), Chinese Academy of Sciences, Ningbo 315201, China

ARTICLE INFO

Article history:
Received 30 December 2019
Received in revised form 28 February 2020
Accepted 11 March 2020
Available online 12 March 2020

Keywords:
Platinum nanodendrites
Hydrogen evolution reaction
Electrocatalytic activity
Long-term durability
pH-universal property

ABSTRACT

High-performance nanomaterial catalysts for hydrogen evolution reaction *via* electrochemical water splitting are significant to the development of hydrogen energy. In this work, we report a robust and highly active catalyst fabricated through direct electrochemical deposition of Pt nanodendrites at the surface of activated carbon (Pt NDs). Owing to the large electrochemically active area and the exposed (111) facet of Pt, Pt NDs exhibits outstanding activity towards hydrogen evolution reaction with a low requiring overpotential of 0.027 V at 10 mA/cm^2 and Tafel slope of ≈ 22 mV/dec in acidic media. In addition, the hydrogen yield of Pt NDs is 30%–45% larger than that of commercial Pt/C at the same Pt loadings. Moreover, Pt NDs exhibits excellent long-term durability whose hydrogen production efficiency remains unchanged after six-hour hydrogen production, while the efficiency of commercial Pt/C catalyst decayed 9% under the same circumstance. Considering the superiority of catalytic activity and stability, this Pt NDs present great potentiality towards practical hydrogen production application.

With the population increasing and economic developing, large demand of energy has become a common problem for human beings. So far, non-renewable fossil fuel occupies 85% of world energy consumption, which contributes to numerous environmental issues, including global warming, acid rain and ozone depletion, *etc.* [1,2]. Under the pressure of resources and environment, it is of great significance to establish a new energy system based on renewable resources [3]. Among renewable resources, hydrogen (H_2) is regarded as a promising alternative to fossil fuel, not only because of its zero-carbon emission but also the high gravimetric energy density (120–142 MJ/kg) [4,5]. Besides, energy conversion between H_2 and electricity can be easily executed through water electrolysis and hydrogen-oxygen fuel cell [6,7]. In order to realize the widespread use of H_2, efficient mass production technologies are needed, including catalytic steam reforming and coal gasification as the representatives [8,9]. As the improvement of solar cell and wind power installation, using H_2 to store surplus solar and wind energy becomes more promising. Therefore, electrochemical water splitting is attracting researchers as a fossil fuel-free strategy to produce H_2 with high purity [9]. To achieve the efficient, stable and scalable electrochemical H_2 production, developing high performance catalysts for hydrogen evolution reaction (HER) is the key point.

In various catalysts, platinum (Pt) is recognized as one of the most effective HER catalyst, which has nearly zero overpotential

* Corresponding author at: Key Laboratory of Marine Materials and Related Technologies, Zhejiang Key Laboratory of Marine Materials and Protective Technologies, Ningbo Institute of Materials Technology and Engineering (NIMTE), Chinese Academy of Sciences, Ningbo 315201, China.
** Corresponding authors.
E-mail addresses: Ljx192665@163.com (J. Liu), tz.wu@siat.ac.cn (T. Wu), linzhengde@nimte.ac.cn (C.-T. Lin).
[1] These authors contributed equally to this work.

https://doi.org/10.1016/j.cclet.2020.03.032
1001-8417/

and outstanding long-term durability [10–12]. However, as a typical noble metal, high cost of Pt makes people seek the alternatives [13]. Over the past decade, with the rise of nanomaterials, many researchers turned their eyes on novel Pt-free HER nanocatalysts [14] to partly replace Pt. On one side, non-noble metals nanomaterials were widely investigated, including transition metal carbides [15–17], chalcogenides [18,19], nitrides [20] and phosphides [21] as well as metal alloys [22]. For example, Yao *et al.* synthesized three-dimensional Ni_2P nanoparticles which exhibited overpotential of 69 mV at 10 mV/cm^2 and Tafel slope of 55 mV/dec in acidic media [23]. Yang *et al.* prepared CoP nanosheet with a Tafel slope of 30.1 mV/dec, which is close to the performance of Pt [24]. On another side, various carbon-based nanomaterials were adopted as metal-free catalyst [25–27]. Although these catalysts are cost saving from the perspective of preparation, they still suffer in high HER overpotential and low hydrogen production efficient, which leads to larger power consumption. Recently, in order to overcome the difficulty, researchers manage to design nanostructure for Pt catalyst to enhance the catalytic property without increasing the yield of Pt [28,29]. For instance, Jiang *et al.* synthesized Pt nanocrystals which achieve a low Tafel slope of 28 mV/dec and large exchange current density of 0.99 mA/cm^2 [30]. Hou *et al.* electro-deposited Pt nanoparticles as HER electrode, whose Tafel slope is estimated to be 53.6 mV/dec [31]. These studies provide inspiration to construct nanostructure of noble metal and indicate that the performance of HER catalyst can be further improved.

In this work, we fabricated nanoscale Pt dendrites at the surface of activated carbon (Pt NDs) by electrodeposition. Obtained Pt nanodendrites exposed numerous atoms at (111) facet which possess better catalytic activity than amorphous Pt [32]. Electrochemical measurements showed that the Pt NDs catalyst exhibits excellent activity with a low Tafel slope (22.2 mV/dec), while that of commercial Pt/C at the same Pt loading is 28.6 mV/dec. Moreover, Pt NDs also displays good electrochemical stability and pH-universal property. Among acidic, neutral and alkaline environment, Pt NDs shows 30%–45% performance enhancement in actual hydrogen production comparing to commercial Pt/C catalyst.

The fabrication process for the preparation of Pt NDs as the hydrogen evolution catalyst was illustrated in Fig. 1a. Firstly, 200 mg activated carbon (AC) powder was dispersed in mixed solvent of 5 mL ethanol and 5 mL de-ionized water by 30-min ultrasonication. Then 500 μL 5% Nafion solution was added into dispersion to form uniform activated carbon ink. 2 μL activated carbon ink was drop-coated and naturally dried at the surface of glassy carbon electrode (GCE) to form the activated carbon electrode. Prior to electrodeposition, Pt chloride solution (10 mmol/L $(NH_4)_2PtCl_6$, 7.5 mmol/L $PtCl_4$, 25 mmol/L NaH_2PO_4, and 425 mmol/L Na_2HPO_4) was prepared and degassed by nitrogen bubbling. A three-electrode system was composed of AC electrode, Pt plate electrode and $Hg/HgCl_2$ electrode as working, counter and reference electrode, respectively. The Pt nanodendrites were electrodeposited onto AC electrode in Pt chloride solution at a constant potential of −0.6 V *vs.* Ag/AgCl for 900 s [33].

The scanning electron microscopy (SEM) images of glassy carbon electrode (GCE), AC layer and Pt NDs are displayed in Figs. 1b–e, which present the change of morphology on the electrode surface. Comparing to smooth surface of GCE as shown in Fig. 1b, AC layer is a sponge-like structure (Fig. 1c), providing significantly larger electrochemically active area [34] as nucleation sites for Pt. Therefore, Pt deposited on AC layer formed nanoscale dendrite structure (Figs. 1d and e), which is beneficial to provide high specific surface area with large amount of active sites and corner atoms. Through energy dispersive spectroscopy (EDS), in-plane elemental mapping of C and Pt of Pt NDs were obtained (Figs. 1f and g), both C and Pt were well distributed, suggesting that our electrodeposition was macroscopically uniform.

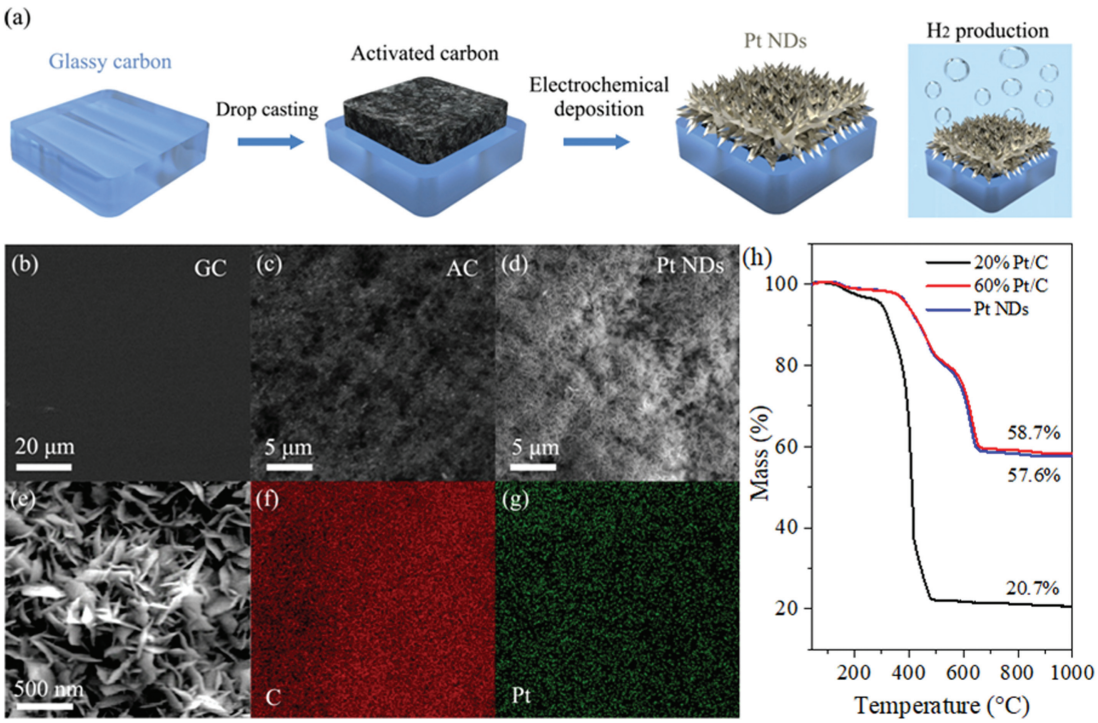

Fig. 1. (a) Scheme of the preparation process of Pt NDs catalyst for hydrogen production. (b–d) SEM top-view images of glassy carbon, activated carbon, and Pt NDs. (e) Regional enlarged view of nanodendrite-structure of (d). (f, g) EDS mapping of element distribution of C and Pt. (h) TGA curves of 20% Pt/C, 60% Pt/C and Pt NDs.

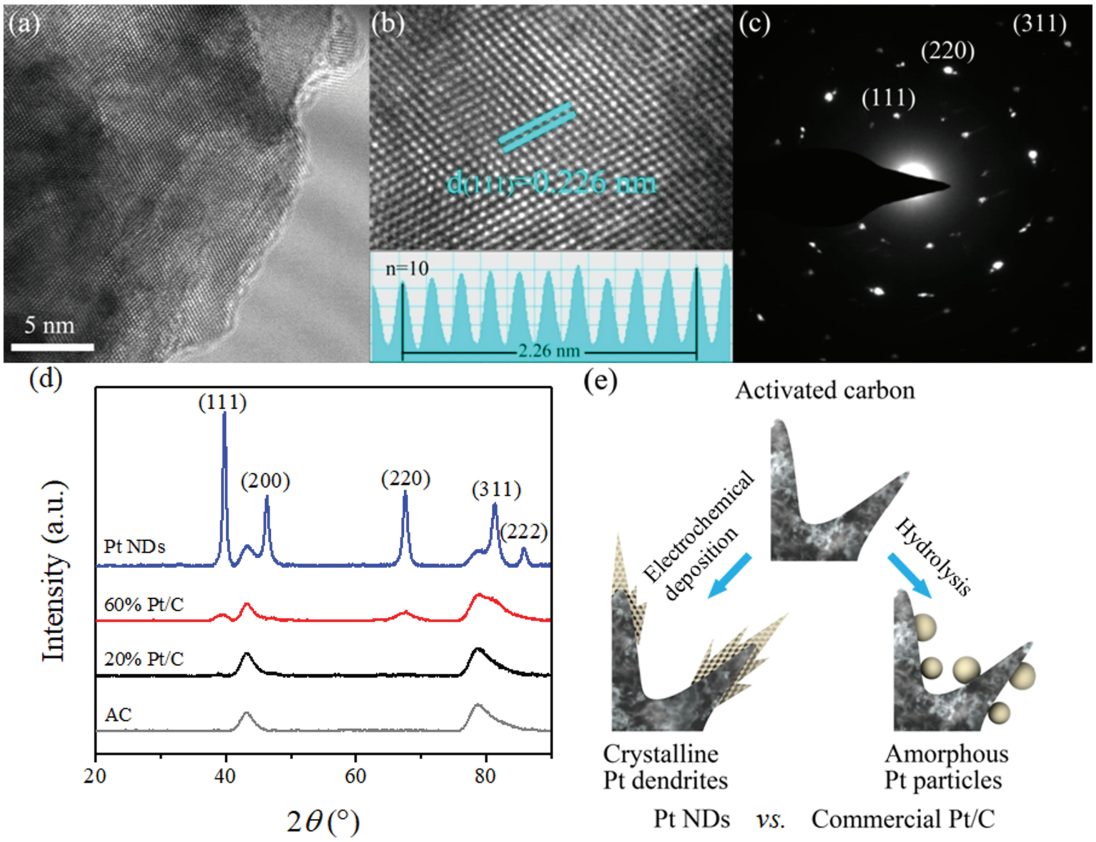

Fig. 2. (a) HRTEM image of representative randomly chosen edge of Pt NDs. (b) SAED patterns of Pt NDs. (c) Atomic image of (a). (d) XRD results of bare AC, 20% Pt/C, 60% Pt/C and Pt NDs. (e) Diagram of the structure difference between Pt NDs and commercial Pt/C.

Thermogravimetric analysis (TGA) was also executed to investigate the deposition mass of Pt. As shown in Fig. 1h, after complete degradation of AC, the mass of residual Pt is 57.6% of the original mass. Considering the Pt mass fraction, we applied commercial 20% Pt/C and 60% Pt/C catalysts (the percentage represents the Pt mass fraction) as control group, whose thermogravimetric analysis (TGA) curves are also shown in Fig. 1h. 20% Pt/C is the most widely used commercial catalyst, and 60% Pt/C has the closest Pt mass fraction to Pt NDs. Note that the curve inflection points reflect the temperature range of carbon degradation. The range of Pt NDs is from 364–663 °C, while that of commercial Pt/C is from 293–485 °C, suggesting that Pt NDs shows better thermal stability. The variation of thermal stability could be attributed to the difference of catalyst structure: Commercial Pt/C catalyst is Pt nanoparticles-loaded carbon structure owing to its hydrolysis preparation process, while Pt NDs has Pt-encapsulated carbon structure formed by electrodeposition which is protective for carbon [35].

In order to get the crystalline information of nanodendrites, Pt NDs was characterized through transmission electron microscopy (TEM). In the TEM bright field image of Pt NDs, although there are some amorphous regions, the overall crystalline of the sample is good and clear lattice fringes can be observed (Fig. 2a). Through counting the lattice fringes in the image with atomic resolution, the spacing of lattice plane is 0.226 nm, corresponding to the (111) facet of Pt (Fig. 2b). The result of selected-area electron diffraction (SAED) measurement shows diffraction patterns of (111), (220), (311) facet of Pt (Fig. 2c). In addition, Pt NDs was also investigated with X-ray diffraction (XRD) using Cu-Kα radiation. As shown in Fig. 2d, five sharp diffraction peaks in Pt NDs are indexed to Pt (111), Pt (200), Pt (220), Pt (311) and Pt (222), respectively, which match well with face-centered cubic (FCC) platinum (PDF No. 04-0802) [36,37]. Two wide peaks are attributed to crystalline carbon in AC [38], which can be also observed in XRD curves of commercial Pt/C catalysts. However, Pt peaks of commercial Pt/C catalysts are unconspicuous compared to Pt NDs. These results proved that Pt atoms deposited on Pt NDs are in good crystallinity, and the preferred lattice plane is (111) facet. In contrast, Pt in commercial Pt/C catalysts is more amorphous, because of their preparation method of precursor hydrolysis (Fig. 2e).

Pt has been regarded as one of the best catalyst for hydrogen production, due to the Gibbs free energy nearest to zero toward HER reaction [32,39]. Moreover, comparing to pure Pt, Pt (111) has larger exchange current in equilibrium, which has been already proved theoretically and experimentally [39–42]. Therefore, we expect that Pt NDs with numerous Pt atoms at (111) facet has higher electrochemical activity than commercial Pt/C. The electrochemical performance of electrocatalysts was measured using a three-electrode system in 0.5 mol/L H_2SO_4. Firstly, the estimation of electrochemical active surface area of 20% Pt/C, 60% Pt/C and Pt NDs was determined *via* the double layer capacitance (C_{dll}) in cyclic voltammetry (CV) curves. Figs. 3a–c show the CV curves of 20% Pt/C, 60% Pt/C and Pt NDs at a series of scan rates (50, 100, 150, 200 and 250 mV/s). The C_{dll} of these catalysts can be determined by plotting the difference of current density at 0.4 V against the scan rate, which is generally proportional to the C_{dll} [43]. According to the results, the C_{dll} of 20% Pt/C, 60% Pt/C and Pt NDs is 3.3, 5.7 and 14.8 mF/cm^2, respectively (Fig. 3d). It demonstrates that C_{dll} of Pt NDs at the similar Pt content is over two times larger than that of 60% Pt/C, indicating that

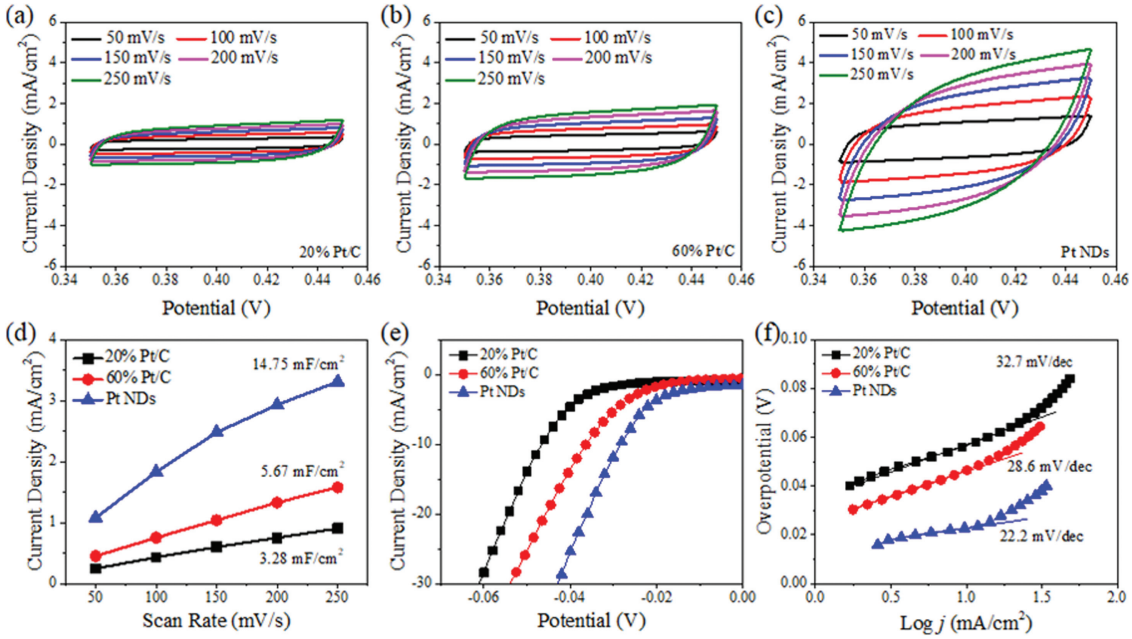

Fig. 3. (a-c) CV traces at different scan rates of 20% Pt/C, 60% Pt/C and Pt NDs, respectively. (d) Capacitive current density as a function of scan rate for 20% Pt/C, 60% Pt/C and Pt NDs. (e) HER polarization curves of 20% Pt/C, 60% Pt/C and Pt NDs. (f) The corresponding Tafel plots derived from (e).

nanodendrite structure could significantly enhance electrochemical active area. Moreover, the linear sweep voltammetry (LSV) was performed to reveal the catalytic activity. As shown in Fig. 3e, the LSV curves shows that Pt NDs requires ultrasmall overpotential of 27 mV to achieve current density of 10 mA/cm^2, while the required overpotentials of 20% Pt/C and 60% Pt/C are 44.6 and 36.3 mV, respectively. A smaller overpotential of Pt NDs among these catalysts suggests a faster increase of HER rate with an increase of applied potential. In order to highlight the merit of Pt NDs, catalytic kinetics was evaluated from the Tafel plots (Fig. 3f) derived from LSV curves. Pt NDs shows a Tafel slope of 22.2 mV/dec, whereas 20% Pt/C and 60% Pt/C exhibit Tafel slopes of 28.6 and 32.7 mV/dec, respectively. The Tafel slope reflects the rate-determining step in catalytic process, while the lowest Tafel slope of Pt NDs indicates that Pt NDs is more active toward the HER. As a consequence, Pt NDs exhibit excellent catalytic activity exceeding commercial Pt/C catalysts, which relies on the crystalline Pt and nanodendrite structure with large surface area.

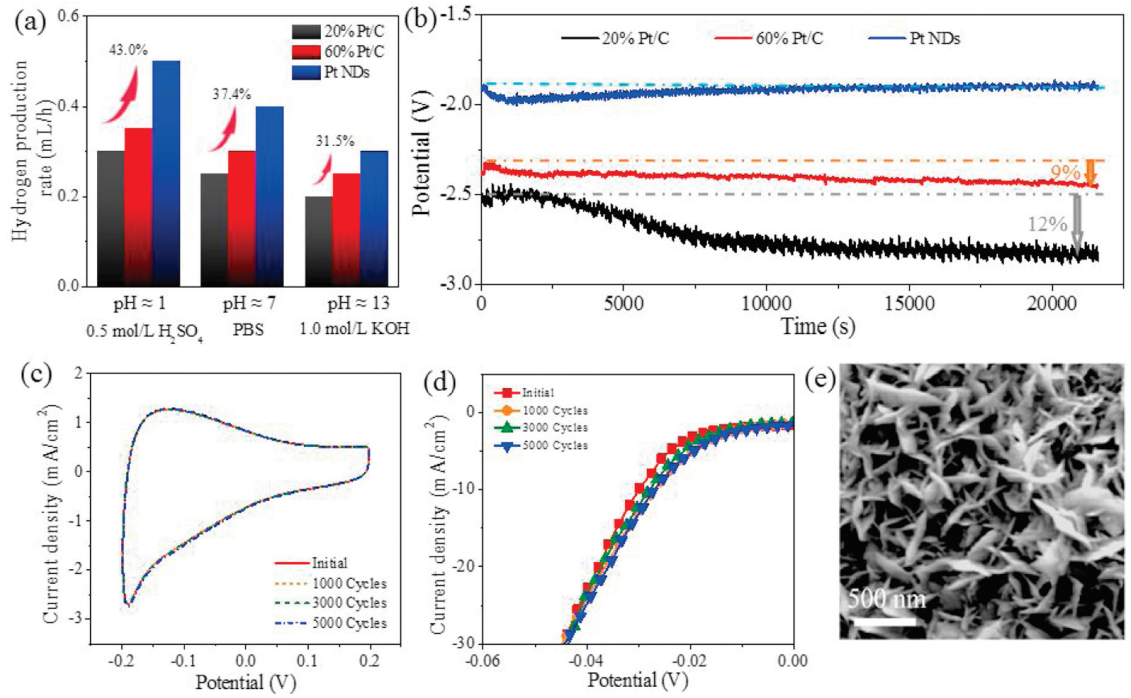

Fig. 4. (a) Hydrogen production rates of 20% Pt/C, 60% Pt/C and Pt NDs in acid, neutral and basic solution, respectively. (b) Results of 6 h galvanostatic test at a constant current density. (c) CV curves of Pt NDs under 1000, 3000 and 5000 cycles CV scanning. (d) HER polarization curves of Pt NDs after CV scanning. (e) SEM images of Pt NDs after electrochemical stability test.

In order to study the actual hydrogen production performance, catalysts are directly used in aqueous media with different pH values under applied voltage at −0.03 V. The quantification of hydrogen gas was executed through drainage water for 5 h after the H_2 was saturated in electrolyte. As shown in Fig. 4a, hydrogen production rate of Pt NDs in 0.5 mol/L H_2SO_4 solution (pH ≈ 1), 1×phosphate buffer saline (pH ≈ 7) and 1.0 mol/L KOH solution (pH ≈ 13) is 0.52, 0.40 and 0.31 mL/h, respectively. The practical efficiency of Pt NDs is 30%–45% higher than that of 60% Pt/C catalysts and 50%–75% higher than that of 20% Pt/C catalysts, suggesting that the nanodendrite structure design shows great potential for HER applications with pH-universal property. Besides, Pt NDs shows excellent stability in long-term galvanostatic test with constant current density of 150 mA/cm^2 in 0.5 mol/L H_2SO_4 solution (Fig. 4b). During the six-hour test, the electrochemical potential of Pt NDs remained almost constant. However, the performance of 20% Pt/C and 60% Pt/C undergo a decay of 12% and 9% after a period of time. It should be noted that hydrogen bubbles generated from commercial Pt/C is larger than those from Pt NDs [44], which can cause physical shock towards catalyst structure, leading to the degradation of catalytic performance. The electrochemical stability of Pt NDs was also investigated by continuous CV scanning. As shown in Fig. 4c, CV curves of Pt NDs remain nearly unchanged even after 5000 cycles. When after 1000 cycles, 3000 cycles and 5000 cycles, LSV tests were also executed and the data can be seen in Fig. 4d. These LSV curves almost overlap with each other and have no difference with initial LSV curves. SEM image of Pt NDs after above tests is similar to initial state as well, suggesting the sample have great morphology stability (Fig. 4e). As a consequence, these findings indicate that Pt NDs not only possesses high catalytic efficiency, but also have outstanding stability under heavy loading.

In summary, we developed Pt nanodendrites at activated carbon catalyst for hydrogen evolution production, which was prepared by electrodepositing Pt onto activated carbon template. Pt NDs exhibits superior catalytic activity with a low overpotential of 0.027 V at 10 mA/cm^2 and a small Tafel slope down to 22.2 mV/dec. This could be attributed to the highly active Pt atoms at preferred (111) facet of the electrodeposited catalyst and large surface area of nanodendrite structure. Besides, Pt NDs could produce hydrogen in aqueous solution with different pH, whose production ratio is 30%–45% higher than that of commercial catalysts at the same Pt loading. Moreover, Pt NDs presents prominent stability even after continuous reacting for 6 h or 5000 CV cycles in 0.5 mol/L H_2SO_4. This work could provide an alternative catalyst and it is expected to be extended to the practical hydrogen production.

Declaration of competing interest

The authors declare that they have no known competing financial interests or personal relationships that could have appeared to influence the work reported in this paper.

Acknowledgments

The authors are grateful for the financial support by the National Natural Science Foundation of China (Nos. 51573201, 51501209 and 201675165), NSFC-Zhejiang Joint Fund for the Integration of Industrialization and Informatization (No. U1709205), the Strategic Priority Research Program of the Chinese Academy of Sciences (No. XDA22000000), Scientific Instrument Developing Project of the Chinese Academy of Sciences (No. YZ201640), Science and Technology Major Project of Ningbo (Nos. 2016S1002, 2016B10038), and International S&T Cooperation Program of Ningbo (No. 2017D10016) for financial support. We also thank the Chinese Academy of Sciences for Hundred Talents Program, Chinese Central Government for Thousand Young Talents Program, and 3315 Program of Ningbo.

References

[1] I. Dincer, Renew. Sust. Energ. Rev. 4 (2000) 157–175.
[2] A. Demirbas, Energ. Source. Part B 1 (2006) 75–84.
[3] A.M. Omer, Renew. Sust. Energ. Rev. 12 (2008) 2265–2300.
[4] S. Dunn, Int. J. Hydrogen Energ. 27 (2002) 235–264.
[5] M. Momirlan, T. Veziroglu, Renew. Sust. Energ. Rev. 6 (2002) 141–179.
[6] L. Zeng, L. Yang, J. Lu, et al., Chin. Chem. Lett. 29 (2018) 1875–1878.
[7] Y. Guo, A. Zhang, C. Li, W. Li, D. Zhu, Chin. Chem. Lett. 29 (2018) 371–373.
[8] R.M. Navarro, M. Pena, J. Fierro, Chem. Rev. 107 (2007) 3952–3991.
[9] J.A. Turner, Science 305 (2004) 972–974.
[10] H. Li, Q. Tang, B. He, P. Yang, J. Mater. Chem. A 4 (2016) 6513–6520.
[11] J. Zheng, Appl. Surf. Sci. 413 (2017) 360–365.
[12] J. Zheng, Y. Zhao, H. Xi, C. Li, RSC Adv. 8 (2018) 9423–9429.
[13] Y. Zheng, Y. Jiao, L.H. Li, et al., ACS Nano 8 (2014) 5290–5296.
[14] E.J. Popczun, C.G. Read, C.W. Roske, N.S. Lewis, R.E. Schaak, Angew. Chem. Int. Ed. 53 (2014) 5427–5430.
[15] W. Zhou, J. Zhou, Y. Zhou, et al., Chem. Mater. 27 (2015) 2026–2032.
[16] S. Wang, L. Zhang, Y. Qin, et al., J. Power Sources 363 (2017) 260–268.
[17] R.A. Mir, O.P. Pandey, J. Clean. Prod. 218 (2019) 644–655.
[18] J.D. Benck, T.R. Hellstern, J. Kibsgaard, P. Chakthranont, T.F. Jaramillo, ACS Catal. 4 (2014) 3957–3971.
[19] Y.R. Liu, X. Shang, W.K. Gao, et al., J. Mater. Chem. A 5 (2017) 2885–2896.
[20] Y. Tian, Y. Ye, X. Wang, et al., Appl. Catal. A: Gen. 529 (2017) 127–133.
[21] Y. Shi, B. Zhang, Chem. Soc. Rev. 45 (2016) 1529–1541.
[22] H. Nady, M. Negem, RSC Adv. 6 (2016) 51111–51119.
[23] Y. Lin, L. He, T. Chen, et al., J. Mater. Chem. A 6 (2018) 4088–4094.
[24] X. Yang, A.-Y. Lu, Y. Zhu, et al., Nano Energy 15 (2015) 634–641.
[25] Y. Jiao, Y. Zheng, K. Davey, S.Z. Qiao, Nat. Energy 1 (2016) 16130.
[26] X. Huang, Y. Zhao, Z. Ao, G. Wang, Sci. Rep. 4 (2014) 7557.
[27] D.Y. Wang, M. Gong, H.L. Chou, et al., J. Am. Chem. Soc. 137 (2015) 1587–1592.
[28] D. Zhou, B. Jiang, R. Yang, X. Hou, C. Zheng, Chin. Chem. Lett. 31 (2020) 1540–1544.
[29] C. Cui, R. Cheng, C. Zhang, X. Wang, Chin. Chem. Lett. 31 (2020) 988–991.
[30] B. Jiang, F. Liao, Y. Sun, Y. Cheng, M. Shao, Nanoscale 9 (2017) 10138–10144.
[31] D. Hou, W. Zhou, X. Liu, et al., Electrochim. Acta 166 (2015) 26–31.
[32] J.K. Nørskov, T. Bligaard, A. Logadottir, et al., J. Electrochem. Soc. 152 (2005) J23–J26.
[33] Q. Zeng, K. Xia, B. Sun, et al., Electrochim. Acta 237 (2017) 152–159.
[34] Y. Chen, Y. Zhang, Y. Lin, et al., Nano Energy 10 (2014) 1–9.
[35] S.P. Ratnayake, N. De Silva, T.K. Kaupuge, et al., Mater. Sci. Eng. B 229 (2018) 59–64.
[36] P. Bera, K. Priolkar, A. Gayen, et al., Chem. Mater. 15 (2003) 2049–2060.
[37] J. Mao, Y. Chen, J. Pei, D. Wang, Y. Li, Chem. Commun. 52 (2016) 5985–5988.
[38] C.G. Kontoyannis, N.V. Vagenas, Analyst 125 (2000) 251–255.
[39] J.K. Norskov, T. Bligaard, J. Rossmeisl, Nat. Chem. 1 (2009) 37–46.
[40] Z. Pu, I.S. Amiinu, Z. Kou, W. Li, S. Mu, Angew. Chem. Int. Ed. 56 (2017) 11559–11564.
[41] R. Subbaraman, D. Tripkovic, D. Strmcnik, et al., Science 334 (2011) 1256–1260.
[42] N.G. Petrik, G.A. Kimmel, J. Chem. Phys. 121 (2004) 3736–3744.
[43] C. Tang, L. Gan, R. Zhang, et al., Nano Lett. 16 (2016) 6617–6621.
[44] Y. Li, H. Zhang, T. Xu, et al., Adv. Funct. Mater. 25 (2015) 1737–1744.